



**Acoustics'08
Paris**
June 29-July 4, 2008

www.acoustics08-paris.org

Time domain modeling of acoustic propagation with acoustic wave propagator and absorbing boundary conditions

Jan Ehrlich

FWG Underwater Acoustics and Marine Geophysics Research Institute, Klausdorfer Weg
2-24, 24148 Kiel, Germany
janehrlich@bwb.org

The acoustic wave propagator (AWP) is the application of the time evolution operator on the acoustic wave equation for stationary systems in a polynomial expansion of Chebyshev polynomials. It allows to increase the time step by more than one order of magnitude compared to finite difference time domain (FDTD) codes. In contrast to other implementations of the AWP the spatial differentiation is carried out with finite difference techniques because this allows the use of the perfectly matched layer formulation as absorbing boundary conditions. The formulation includes the direct implementation of acoustic sources with sinusoidal time evolution. Other sources can be synthesized by their Fourier components. For the calculation of large areas the explicit formulation of a large system matrix can be avoided by calculating the propagation equations for each time step at row and column level repeatedly which reduces memory requirements notably. This procedure and the suitability of the finite difference approach for parallelization makes the extension to fully three dimensional calculations possible. Examples for benchmark problems with sound propagation in air and water are given.

Introduction

Over many years finite difference time domain (FDTD) schemes have been very popular for the numerical simulation of acoustic propagation in the time domain. The method is widely used because it is simple to implement and it can cover a wide range of applications. The use of the perfectly matched layer (PML) boundary as an efficient absorbing boundary condition for open space propagation has increased its popularity. One of the drawbacks of FDTD codes is the coupling between the spatial step size and the step size in time by the sound speed and the Courant number. This leads to very short time steps in order to maintain stability. An efficient way to overcome this problem is the propagator concept that was originally introduced by Tal-Ezer and Kosloff [1] to solve the time dependent Schrödinger equation in quantum mechanics and was transferred to the acoustic wave equation by Pan and Wang [2,3] who named the method acoustic wave propagator (AWP). This method for solving time dependent wave equations for systems with stationary coefficients has theoretically no limit for the time step and practically allows time steps much larger than FDTD codes.

Acoustic propagator

Formulation

The linearized acoustic wave equation can be written as a system of two first order partial differential equations with the quantities pressure p and velocity \vec{v} and the material parameters sound speed c and mean density ρ_0

$$\begin{aligned} \frac{\partial}{\partial t} p + \rho_0 c^2 \vec{\nabla} \cdot \vec{v} &= 0 \\ \frac{\partial}{\partial t} \vec{v} + \frac{1}{\rho_0} \vec{\nabla} p &= 0 \end{aligned} \quad (1)$$

In compact notation this system of PDEs can be written as

$$\frac{\partial}{\partial t} \phi + \mathbf{H} \cdot \phi = 0 \quad (2)$$

with p and \vec{v} written in vector notation as ϕ and the matrix operator \mathbf{H} containing the spatial derivative operator that will be applied to pressure and velocity.

$$\phi = \begin{pmatrix} p \\ \vec{v} \end{pmatrix}, \quad \mathbf{H} = \begin{pmatrix} 0 & \rho_0 c^2 \vec{\nabla} \cdot \\ 1/\rho_0 \vec{\nabla} & 0 \end{pmatrix} \quad (3)$$

Eq.(2) can be solved formally as

$$\phi(x, t) = e^{-\mathbf{H}(t-t_0)} \cdot \phi(x, t_0) \quad (4)$$

under the assumption that the operator \mathbf{H} is not time dependent. This is the case for stationary acoustic problems with material parameters c and ρ_0 being constant in time, but not necessarily in space. Eq.(4) describes the time evolution of the system starting from the known state at time t_0 to time t .

The actual calculation of the solution is carried out by the expansion of the operator $e^{-\mathbf{H}(t-t_0)}$ in a polynomial series with terms of matrix \mathbf{H} . Especially well suited is an expansion with Chebyshev polynomials as

$$e^{-\mathbf{H}(t-t_0)} = \sum_{k=0}^{\infty} \alpha_k I_k(t-t_0) T_k(\mathbf{H}') \quad (5)$$

with $\mathbf{H}' = \mathbf{H}/|\lambda_{\max}|$ being matrix \mathbf{H} normalized by its maximum eigenvalue. T_k denominates the Chebyshev polynomials and I_k stands for the modified Bessel functions of first kind and k -th order. Constants a_k are $a_k = 1$ except for $a_0 = 2$. The Chebyshev polynomials are recursively defined as $T_{k+1}(\mathbf{H}') = 2 \mathbf{H}' T_k(\mathbf{H}') - T_{k-1}(\mathbf{H}')$ and $T_0(\mathbf{H}') = \mathbf{1}$, $T_1(\mathbf{H}') = \mathbf{H}'$

The recursive definition of the Chebyshev polynomials has the convenient effect that for the calculation of the expansion in Eq.(4) the term of order $k+1$ can be calculated with just one multiplication by the matrix \mathbf{H}' . In the actual code this amounts not even to a matrix-matrix multiplication but just a matrix-vector multiplication since the operator is always applied to the state vector ϕ .

Theoretically there is no limit for the time step size $(t-t_0)$. But practically the representation of the floating point number in the computer limits the time step size. Without special emphasis to this point increase in the order of factor 10-20 could be reached for the examples presented in section 3.

In an implementation on a computer the series of Eq.(5) has to be truncated after convergence is reached. But the number k necessary for convergence depends on the step size $(t-t_0)$. The series of products $I_k \cdot T_k$ is made up of progressively increasing terms of alternating positive and negative sign before converging to the result for the time step in question. Thus a limit of k has to be set in order not

to reach the limit of precision in double precision floating point arithmetic. In practice the limit depends on the numbers in the matrix **H** and is therefore determined by the material parameters and the size of the calculatory domain.

Spatial derivatives

For the evaluation of the spatial derivative this scheme uses a finite difference approach. Pan *et al* [2,3] have proposed a scheme with pseudospectral derivatives which is certainly more accurate, but has the drawbacks that the PML boundary can apparently not be applied satisfactorily and additional precautions have to be taken to avoid Gibbs' phenomenon at discontinuities of the material parameters.

The scheme uses the staggered grid of Yee [4] with the evaluation points for pressure and velocity separated by half a step shown in Fig.1. The staggered grid ensures that the chosen approximated derivative with the next neighbors only

$$\frac{\partial p(x_{i+1/2})}{\partial x} \approx \frac{p(x_{i+1}) - p(x_i)}{\Delta x}, \quad i = 1, \dots, N \quad (6)$$

$$\frac{\partial v_x(x_i)}{\partial x} \approx \frac{v_x(x_{i+1/2}) - v_x(x_{i-1/2})}{\Delta x}, \quad v_{1/2} = v_{N+1/2} = 0$$

has second order accuracy. Δx is the spacing between points of the same type (e.g. pressure) and not between points of pressure and velocity. Higher order approximations have produced inaccuracies at interfaces between different media.

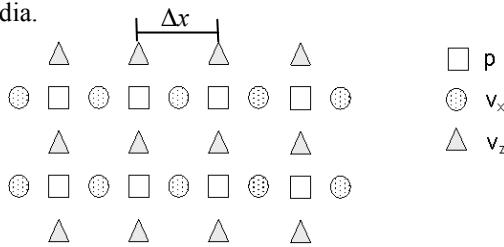


Fig.1 Calculation grid for 2 dimensions with grid points for p, v_x and v_z separated by half the spatial step size.

The calculation of large areas can be facilitated by an implementation that never actually formulates matrix **H** but calculates the needed derivatives of pressure and velocity for each point and each application of the matrix on the vector ϕ . This procedure drastically reduces the demand of computer memory and thus makes calculations of large areas possible. It requires only scalar multiplications instead of matrix vector products. On the other hand the number of multiplications needed is much higher which leads to an overall increase of computing time roughly by a factor of 2 in a Matlab implementation.

The accuracy of the scheme could be increased by the use of better spatial differencing methods, probably at the expense of coding simplicity, memory requirements and run time though.

PML boundaries

In order to ensure low reflections from the borders of the calculatory domain the Perfectly Matched Layers (PML) boundaries according to Bérenger [5] are used. This is a

standard technique in FDTD codes that produces low reflections by adding artificially damped regions at the edges of the calculatory domain. In spite of the increased demands in computer memory Bérenger's original split-field formulation was used rather than stretched coordinate formulation of the PML because it is simple to code and integrates well into the matrix formulation. In the split field formulation pressure p is artificially separated in p_x and p_z in the PML regions and only the components perpendicular to the respective edge are damped. In two dimensions this leads to a system of 4 equations instead of the three equations of Eq.(1)

$$\begin{aligned} \frac{\partial p_i}{\partial t} + q_{pi} p_i + c_0^2 \rho_0 \frac{\partial v_i}{\partial x_i} &= 0 \\ \frac{\partial v_i}{\partial t} + q_{vi} v_i + \frac{1}{\rho_0} \frac{\partial p}{\partial x_i} &= 0 \end{aligned} \quad i = (x, z) \quad (7)$$

with the damping parameters q_{pi} and q_{vi} and the observable quantity pressure p in the PML region being the sum of the artificially separated values p_x and p_z .

In the matrix **H** the damping terms lead to additional terms on the main diagonal in the damped regions. The damping factors q_{pi} and q_{vi} were chosen with polynomial growth starting from the beginning of the damped region at x_{ig}

$$q_{pi}(x_i) = q_{p0} \left(\frac{x_i - x_{ig}}{\Delta R_i} \right)^\alpha \quad (8)$$

ΔR_i is the width of the PML boundary in the x_i direction.

For water as fluid good results were achieved with values of $q_{p0} = 750 \text{ kg}/(\text{m s}^3)$ and exponent $\alpha = 2.5$ and a width of the PML boundary of approximately one wavelength.

Three-dimensional formulation

Eq.(1) describes the problem in Cartesian coordinates in either two or three dimensions with p, v_x, v_z (and v_y in 3 dimensions). For three dimensional calculations the demand for computer memory and calculation time rises enormously. For the special case of rotationally symmetric problems this can be avoided by a formulation in cylindrical coordinates which keeps the problem mathematically two-dimensional. The only difference is an additional term in the Euler equation (Eq.(1) upper equation) which is replaced by

$$\frac{\partial}{\partial t} p + \rho_0 c^2 \frac{v_r}{r} + \rho_0 c^2 \vec{\nabla} \vec{v} = 0 \quad (9)$$

and the notion that the velocity \vec{v} now consists of the components v_z in z direction and v_r in radial direction. Consequently the spatial derivative operator is now defined as $\vec{\nabla} = (\partial/\partial r, \partial/\partial z)$.

Acoustical sources

In the presence of an acoustical source Eq.(2) is modified with a source term $\vec{S}(x, t)$ on the right hand side. The solution of the resulting equation is found as

$$\bar{\phi}(x,t) = e^{-\mathbf{H}(t-t_0)} \cdot \bar{\phi}_0(t_0) + \int_{t_0}^t e^{-\mathbf{H}(t-t')} \cdot \bar{S}(x,t') dt' \quad (10)$$

For a source with a sinusoidal time evolution $\bar{S}(x,t) = \bar{\sigma}(x) \cdot \sin(\omega t)$ this integral can be solved analytically as

$$\int_{t_0}^t e^{-\mathbf{H}(t-t')} \cdot S(x,t') dt' = (\mathbf{H}^2 \omega^2)^{-1} [-e^{-\mathbf{H}(t-t_0)} (\mathbf{H} \sin(\omega t_0) - \omega \cos(\omega t_0)) + \mathbf{H} \sin(\omega t) - \omega \cos(\omega t)] \sigma(x) \quad (11)$$

Sources with a different time evolution can be synthesized by their Fourier components. In order to calculate the spatial derivatives properly the source has to be modeled as a small area rather than a single point.

Examples

In this chapter three examples of the code are presented. The first is a two-dimensional calculation with a sinusoidal source compared to the pressure field of a two-dimensional analytic point source. The second example shows a snapshot of the evolution of one sinus-pulse in a layered medium consisting of water, air and a sloped sediment. The third example gives a comparison with a frequency domain calculation for another layered medium.

Fig.2 shows the pressure field of a sinusoidal source with a frequency of 150 Hz at a depth of 50 m after 100 ms in a two-dimensional calculation. The horizontal black lines at $z = 0$ m, $z = 100$ m and the vertical line at $x=200$ m mark the beginning of the damped PML domains.

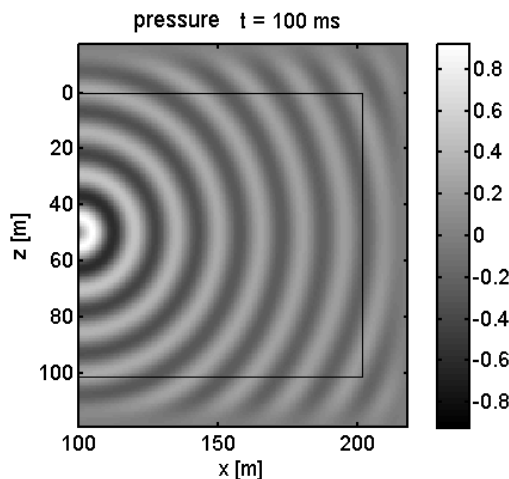


Fig.2 Sinusoidal 2D source in water.

A comparison of the pressure on a horizontal line at source depth with the analytical solution of a point source at the same position (dotted line) is presented in figure 3. In the near-field the differences between the simulated, extended source and the idealized point source is clearly visible. In the far field after approximately 10 wavelengths the pressure field is virtually identical for the two cases.

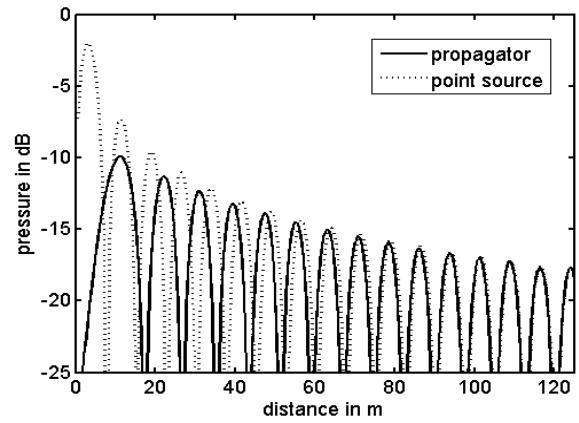


Fig.3 Comparison with point source.

Figure 4 shows a snapshot of a short pulse with one 150 Hz sine wave in a three-dimensional calculation with rotational symmetry after 500 ms on a logarithmic scale.

The medium is layered with air on top, water in the middle and a sloped sediment beneath. The source was located in the water at a depth of 150 m.

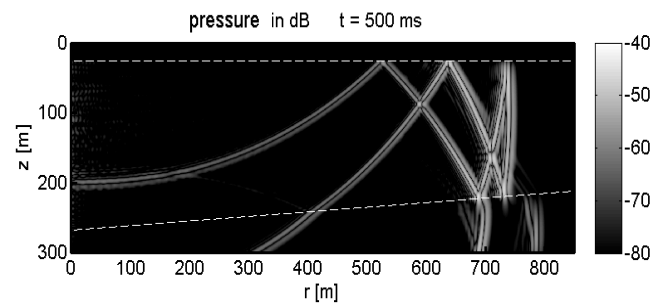


Fig.4: Pulse in layered medium (air /water/sediment).

The sediment is modeled as a fluid and not as a solid. The PML regions are not shown in this figure. The dotted lines mark the interfaces between the air, water and sediment.

The reflections of the pulse from the interface with the air layer and the sediment can be observed. A part of the energy was injected in the sediment region and propagates with higher sound speed.

Fig.5 shows the results of a different calculation with another layered medium with a 40 Hz sinusoidal source in the air. The position of the source was at 50 m, the horizontal interfaces were at 100 m (air/water) and 200 m (water/sediment). The calculation covered the time up to 1.7s so that a stationary state has been reached in the entire domain. The results show phase fronts propagating through the medium with maximum amplitudes constant in time for each point. The maximum amplitudes, normalized with the source strength, are equal to the transmission loss in the computational domain (Fig.5). The calculation shows the grating lobe pattern in the air produced by the partial reflection at the interface and the cone beneath the source where sound is introduced into the water. For shallower angles at larger distances the conditions for total reflection according to Snell's law are met and sound is only introduced into the water via the evanescent wave at the interface that can also be observed.

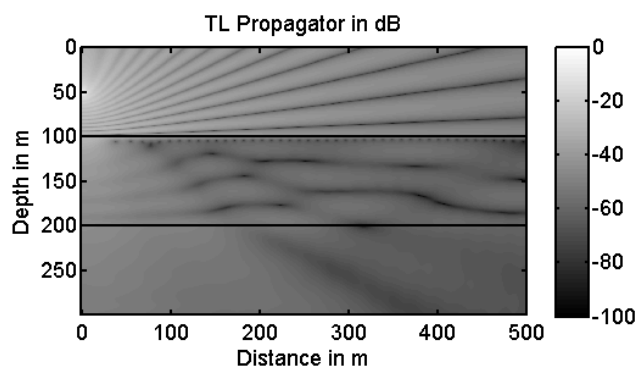


Fig.5 Transmission loss in a layered medium in dB.

These results were compared to an analytical calculation of the transmission loss in frequency domain with a Green's function approach. Figure 6 shows the differences between the two calculations in dB. The results were normalized to produce the same value at the point 10 m to the right of the source in order to avoid the nearfield discrepancies caused by the different source formulations.

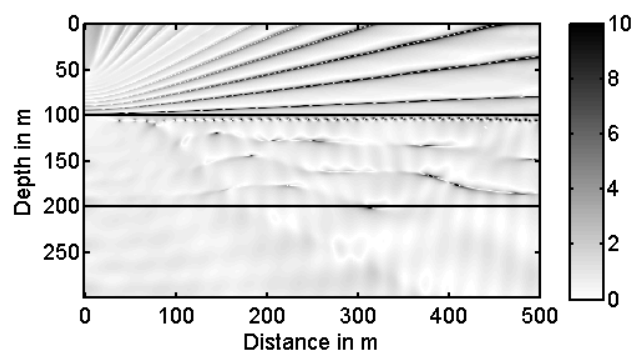


Fig.6 Difference between propagator calculation and analytical solution in the frequency domain in dB.

The differences between the results of the propagator scheme and the analytical calculation are below 1 dB for most of the calculatory domain. Exceptions are the locations of the minima in air and water. These strong minima, however, are very sensitive to small differences in the calculations and would not be measured to that extent in an actual measurement with background noise.

Compared to a frequency domain method the calculation for this example needed much more time (several hours). But such a harmonic problem is not the typical application for a time domain code that is best suited for the calculation of short pulses. This example was just included for the comparison of the results of the quasi stationary that was reached in the time domain.

5 Conclusion

The acoustical wave propagator provides a method to increase the time step size for time domain calculations of acoustic propagation. With spatial derivatives formulated by finite difference methods it gives an efficient scheme to accurately calculate large domains in two dimensions and problems in three dimensions with rotationally symmetry. The formulation allows the use of the efficient PML boundary conditions as termination to simulated free field

conditions. Acoustic sources can be included in the formulation. Results were presented that show good agreement with analytical calculations both in time domain and in frequency domain for a simulation of a stationary acoustic field with a continuous monofrequent source. Compared to FDTD computations increases in the order of one magnitude could be reached in the time step size, depending on the material parameters of the problem and the size of the computational domain.

References

- H. Tal-Ezer, R. Kosloff, "An accurate and efficient scheme for propagating the time-dependent Schrödinger equation", *J. Chem. Phys.* 81, 3967-3971 (1984)
- J. Pan, J.B. Wang, "Acoustical wave propagator", *J. Acoust. Soc. Am.* 108, 841-847 (2000)
- J. Liu, J. Pan, B. Xu, "Time domain calculation of acoustical wave propagation in discontinuous media using acoustical wave propagator with mapped pseudospectral method", *J. Acoust. Soc. Am.* 118, 3408-3419 (2005)
- K. S. Yee, "Numerical solution of inertial boundary value problems involving Maxwell's equation in isotropic media", *IEEE Antennas Propagat.*, 14 (3), 302-307, (1966)
- J. P. Bérenger, "A perfectly matched layer for the absorption of electromagnetic waves", *J. Comput. Phys.* 114 (2), 185-200 (1994)